PERGAMON

International Journal of Heat and Mass Transfer 45 (2002) 3223–3231

International Journal of HEAT and MASS TRANSFER

www.elsevier.com/locate/ijhmt

Heat transfer characterization of support structures for catalytic combustion

Andreas Brautsch [a,1], Timothy Griffin [a,*], Andreas Schlegel [b]

[a] *ALSTOM Power Technology, CH-5405 Baden-Dättwil, Switzerland*
[b] *awtec AG, CH-8050 Zürich, Switzerland*

Received 27 July 2001

Abstract

Convective heat transfer and pressure drop characteristics within metal foil catalyst structures are determined with a unique experimental procedure. Various honeycomb-type structures with 100, 150, 160 and 200 cpsi (cells per square inch) are investigated at empty tube air velocities ranging from 0.5 to 10 m/s at atmospheric pressure. Both commercially available and novel structures, designed and manufactured by the authors, are compared. The convective heat transfer between fluid and substrate can be well described by the correlation $Nu = \phi Re^m Pr^{1/3}$. The experimental method to obtain values of ϕ and m is described in detail and is based on unsteady state cooling of the hot structures in an air stream. The data are discussed in view of application of the structures as catalyst supports and are compared with a 400 cpsi conventional, parallel-channel, Cordierite honeycomb. Results show that the novel structures offer greater heat transfer per unit volume but at the cost of higher pressure drop and thus lower heat transfer per unit pressure drop, relative to the 400 cpsi, parallel-channel honeycomb. © 2002 Elsevier Science Ltd. All rights reserved.

Keywords: Experimental; Measurement; Heat transfer; Combustion; Energy

1. Introduction

This report summarizes the characterization of heat transfer and pressure drop for various metal foil structures. These structures can be used as catalyst supports for catalytically stabilized combustion, a process for reducing NO_x emissions in gas turbines [1,2].

All structural designs of catalyst supports aim for low pressure drop combined with favorable transport properties. This report concentrates on the examination of corrugated metal foil catalyst structures, manufactured in the form of honeycombs, that provide both a large number of channels in the flow direction and a high specific surface area. These structures are corrugated in a novel fashion to provide additional turbulence within the flow field. Due to the relatively high thermal conductivity of metal foils in comparison to ceramic materials, localized areas of high temperature (hot spots) can be reduced. Additionally, with metal foils the catalyst may be coated only on one side of the foil surface, allowing a passive cooling effect as described in US Patent 5′202′303.

However, reliable transport properties are not generally available for such structures. Facilities were thus designed to examine transport properties and pressure drop in both commercially available and self-made metal foil structures. Experimental results are discussed and compared with data of conventional, parallel-channel, ceramic honeycombs [3,4]. The results for heat and mass transfer are combined with the associated pressure drop values of the different packings to rate their ''efficiency''. The aim is to identify a catalyst support structure with optimized heat transfer and pressure drop over the catalyst's length.

* Corresponding author. Tel.: +41-56-486-8243; fax: +41-56-486-7389.

E-mail address: timothy.griffin@power.alstom.com (T. Griffin).

URL: www.alstom.com, www.awtec.ch

[1] Currently at Department of Mechanical and Chemical Engineering, Heriot-Watt University, Edinburgh, UK.

0017-9310/02/$ - see front matter © 2002 Elsevier Science Ltd. All rights reserved.
PII: S0017-9310(02)00029-7

Nomenclature

a	specific surface (m^2/m^3)
Bi	Biot number (dimensionless)
c	specific heat (J/kg K)
$¢$	constant in heat transfer correlation (dimensionless)
d_h	hydraulic diameter (m)
D	packing diameter (m)
D_{eff}	effective packing diameter (m)
L	length (m)
m, n	exponents in heat transfer correlation (dimensionless)
M	mass flux (g/s)
Nu	Nusselt number (dimensionless)
Δp	pressure drop (Pa)
Pe	Peclet number (dimensionless)
Pr	Prandtl number (dimensionless)
q	heat flux (W/m^2)
Re	Reynolds number (dimensionless)
T	temperature (°C, K)
T_{in}	inlet temperature (°C, K)
T_{mean}	mean temperature (°C, K)
T_{out}	outlet temperature (°C, K)
T_0	initial packing temperature (°C, K)
t	time (s)
t_{wall}	wall thickness (m)
v	velocity (m/s)
v_0	empty tube velocity (m/s)
V	packing volume (m^3)
x	axial coordinate (m)
α	heat transfer coefficient (W/m^2 K)
ϵ	porosity (%)
η	dynamic viscosity (kg/m s)
λ	thermal conductivity (W/m K)
ρ	density (kg/m^3)
Subscripts	
f	fluid
s	solid
x	axial direction

2. Experimental method to determine transport coefficients

2.1. Overview

Different techniques to ascertain heat and mass transfer properties in catalyst packings are known from the literature [3,5]. The majority of such suffer from being both complicated and costly, especially where mass transport properties are concerned.

In contrast, a relatively simple and accurate method to determine heat transfer coefficients has been developed [6]. A constant flow rate of air is maintained through the catalyst structure, also referred to as the packing, and a step-like change of the airflow temperature is applied to the system. Air temperatures are recorded as a function of time at the inlet and outlet of the packing. These measured temperature curves are analyzed iteratively, using a one-dimensional heat transfer model to determine the heat transfer coefficient. By applying the analogy of heat and mass transfer, mass transfer coefficients can also be obtained. The above-mentioned, step-like temperature change is imparted upon the system by means of a catalytic pre-burner placed upstream of the investigated packing, as shown in Fig. 1. The pre-burner consists of a lightweight metal foam coated with palladium catalyst. Hydrogen is added to the airflow and fully oxidized on the pre-burner

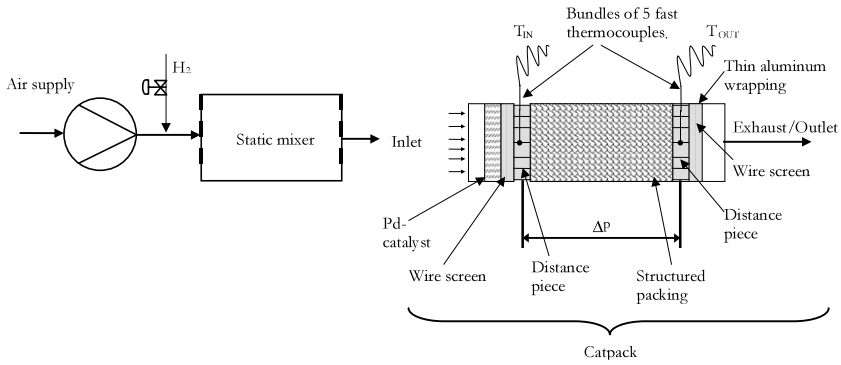

Fig. 1. General layout of the experimental set-up: heat transfer test rig.

catalyst, heating up the airflow to a temperature of approx. 300 °C. At steady state conditions, the hydrogen supply is rapidly switched off so that a sudden, almost step-like air temperature drop at the inlet of the packing is achieved. An ordinary heater, such as an electrical pre-heater, would not be suitable for this purpose due to its high thermal inertia. In this case it would be necessary to by-pass the flow to achieve such a quick temperature change, which would, in turn, generate unacceptable fluctuations in flow rate and pressure.

The methodology applied in this work to determine heat transfer properties in catalyst packings comprises three tasks:

- Measurement of gas flow temperatures as a function of time (Section 2.2).
- Numerical simulation of the measurements (Section 2.3).
- Iterative determination of heat transfer coefficients with the model until experimental and theoretical results converge (Section 2.3.1).

2.2. Experimental work

2.2.1. Experimental set-up

A module called "Catpack" (Fig. 1) containing the catalyst support structure is inserted into the test rig used for measurement of heat transfer properties. A mass flow controlled blower supplies constant airflow to which hydrogen is added upstream of the Catpack. A homogeneous distribution of fuel in the bulk flow is ensured with a static mixer (Sulzer SMV). At the inlet of the Catpack, hydrogen is oxidized completely in a lightweight metal-foam catalyst, which responds quickly to changes in hydrogen flow. This method allows for an almost step-like temperature change at the inlet of the investigated packing when the hydrogen supply is suddenly turned off. The pressure drop (Δp) over the packing length is measured by means of small pressure taps at the inlet and the outlet section of the Catpack.

The "Catpack" set-up is designed to attain quasi one-dimensional flow conditions ("plug-flow" with a uniform temperature over the cross-section of the packing), such that a one-dimensional mathematical model can be employed. Bundles of five thermocouples, located at the center of the packing, are installed at the inlet and outlet of Catpack, spread over a diameter of approx. 20 mm. The influence of the outer wall of the Catpack is negligible in this center region where a one-dimensional description is valid. Cr–Ni alloy, type K thermocouples are used with 0.5 mm sheath diameter and exposed tips (diameter 0.1 mm), resulting in quick response times. A corrugated circular distance piece, located at the inlet and at the outlet of the packing, acts as a spacer for the bundles of thermocouples. A wire screen consisting of five layers of stainless steel mesh 100 is mounted between the Pd-catalyst and the inlet thermocouples, and also between the outlet thermocouples and the exhaust tube, so as to minimize radiation effects and to achieve plug flow conditions.

The Catpack assembly is wrapped in a thin ceramic fiber mat to prevent flow by-pass, and then in a 0.3 mm thick aluminum foil. The wrapping is assumed to have negligible influence on the heat transfer measurements in the packing due to its low thermal mass.

Additionally, since T_{in} is not higher than 300 °C, only small heat losses to the surroundings through convection and radiation occur. The mass flow of hydrogen is adjusted with a needle valve to stabilize the temperature T_{in} at about 300 °C. After reaching steady state conditions at a specific airflow, the hydrogen supply is turned off instantaneously and all temperatures are recorded in half-second intervals. The readings of the inlet and outlet thermocouple bundles are averaged to account for scattering in the measurements. Sample results showing the average responses of inlet and outlet temperatures for two different mass flows are given in Fig. 2.

The above procedure is repeated for different mass flows ranging from 10 to 75 g/s of air at atmospheric pressure.

2.2.2. Examined structures

Structures manufactured with three different metal foil corrugation patterns were examined. First, the "Herringbone" structure, with the flat foil supplied by Texas Instruments (TI) and the corrugations added by Engelhard Corporation, is shown at the top of Fig. 3. With this design the flow direction changes several times by an angle of approx. 9°. A completely different approach is the Skew pattern corrugation as shown in the middle of Fig. 3 where the corrugations are "skewed"

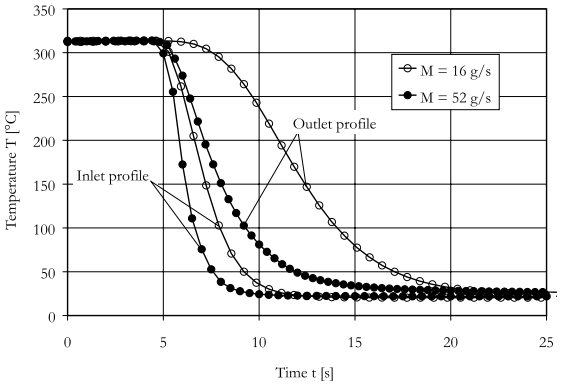

Fig. 2. Experimental results for the fluid temperature at the inlet and at the outlet of a 150 cpsi Herringbone TI packing for two different mass flows of air.

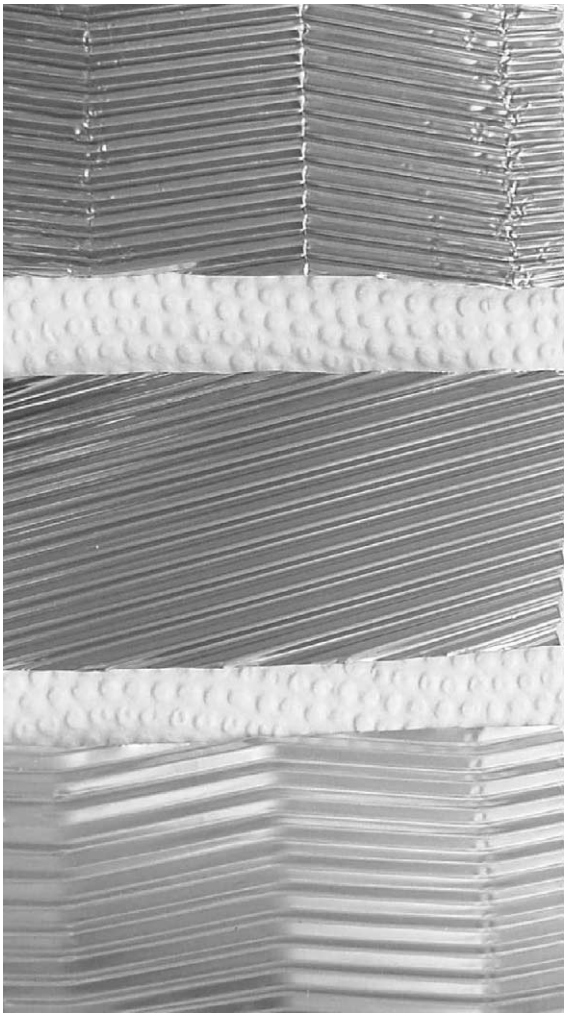

Fig. 3. Corrugation patterns employed in the manufacture of catalyst support structures: 150 cpsi Herringbone TI (top), 100 cpsi Skew pattern (middle) and TI 160 cpsi Herringbone APT SK (bottom).

with respect to the main flow direction. Engelhard also provided these foils.

The authors at ALSTOM Power Technology (APT) modified the existing Herringbone shape by corrugating the foil with a different tool, thereby avoiding abrupt deformations at the transition points, as shown at the bottom of Fig. 3 (Herringbone APT SK). Steel foil provided by SANDVIK (SK) has been used for the Herringbone APT SK structure.

A cylindrical catalyst packing is formed by rolling two layers of the above mentioned metal foils oriented in opposite directions around a central rod (mandrel) as shown in Fig. 4. The patterns of the two foils have to be oriented in opposite directions to avoid nesting, so that channels emerge. For the heat transfer tests the central

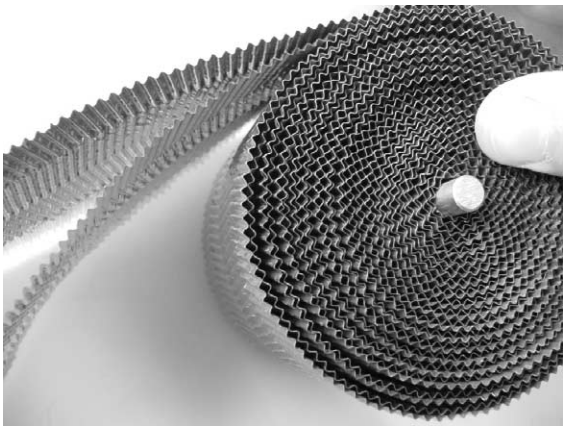

Fig. 4. Catalyst support structure comprised of multiple layers of "Herringbone"-corrugated foil.

mandrel was removed, due to its high thermal mass. The resulting hole was filled in with heat resistant silicon paste.

Due to the "zig-zag" nature of the channels formed in the structures, fluid flow passing through the structure has to change its direction several times. This leads to enhanced (as compared to straight channels found in ceramic honeycombs) mixing inside the packing due to induced turbulence and radial fluid exchange. Both Herringbone and Skew pattern structures have been tested with different cell densities. By decreasing the wavelength of the corrugation, the cell density of the packing can be increased to form catalyst supports with higher specific surfaces. The cell density obtained with a given wavelength foil lies within a range of values because it depends strongly on the rolling process (deviation from the mean value $\pm 5\%$). Tables 1 and 2 provide information on geometrical data and material properties of all examined structures.

Use of the ceramic fiber mat causes the outer cells of the packings to be blocked, thereby reducing the diameter, D, to the effective diameter, D_{eff}, by approx. 2 mm. All data (empty tube velocity v_0, Reynolds number, etc.) are thus related to the effective diameter D_{eff} of the packing.

The hydraulic diameter d_{h} and channel Reynolds number Re are defined according to Eqs. (1) and (2):

$$d_{\mathrm{h}} = 4\,\frac{(V/L)\,\varepsilon}{(V\,a)/L} = 4\,\frac{\varepsilon}{a}, \tag{1}$$

$$Re = \frac{\rho_{\mathrm{f}}\,v_0\,d_{\mathrm{h}}}{\varepsilon\,\eta_{\mathrm{f}}}, \tag{2}$$

where the empty tube velocity v_0 is related to D_{eff}. During the experiments the flow velocity (based upon air at 20 °C and atmospheric pressure) was varied between 2 and 9 m/s, resulting in the Reynolds number range shown in Table 1.

Table 1
Geometric data and *Re* number ranges for the examined structures

	Re (dimensionless)	ε (%)	a (m^2/m^3)	d_h (mm)	D (mm)	D_{eff} (mm)	L (mm)
100 cpsi HB TI	380–1560	95.7	1682	2.28	75	73	89
150 cpsi HB TI	290–950	94.9	2095	1.81	75	73	89
200 cpsi HB TI	210–1130	94.3	2453	1.54	75	73	89
100 cpsi SP TI	270–1250	95.6	1680	2.28	75	73	89
160 cpsi HB APT SK	240–1130	94.5	2125	1.78	75	73	89
400 cpsi monolith	52–2112	82.7	2620	1.083	75	73	2×75

Table 2
Material properties of the tested structures

	Texas instruments (TI)	Sandvik (SK)	Monolith
Composition (kg/kg)	Fe 72.8/Cr 22/Al 5/Y 0.1/Zr 0.1	Fe 74.96/Cr 20/Al 5/Y 0.2/C 0.02	Cordierite
Density ρ (g /cm^3)	7.22	7.3	2.51
Thermal conductivity λ @RTP (W/m K)	16	12	2.46
Thickness t_{wall} (mm)	0.05	0.05	0.2
Melting point (°C)	1380–1490	1470	1450

2.3. Theoretical model

To fully describe heat transfer between fluid and solid in packed beds, a heterogeneous two-phase model with varying material properties would have to be employed [6]. In order to simplify the model, the following assumptions are made:

- The flow and temperature fields are one-dimensional, according to the experimental set-up.
  Thus, plug flow conditions are valid and fluid and solid temperatures vary in the axial direction only ($T_f, T_s = f(x)$).
- Conductive heat transfer in the axial direction in the fluid ($Pe \gg 1$) and in the solid is negligible.
  Numerical results for Cordierite honeycombs showed that the calculated heat transfer coefficient changed by less than 1% when conduction in the solid was taken into account [7]. Using metal foil as a support structure, the higher thermal conductivity is compensated by the smaller material thickness (Table 2).
- Heat transfer between solid and fluid can be described solely by convective heat transfer as in Eq. (3):

$$q = \alpha(T_s - T_f), \tag{3}$$

  where T_f is the bulk fluid temperature and T_s the solid temperature. T_s is assumed to be constant over the cross-section of the metal foil, i.e. the conductive thermal resistance in the solid perpendicular to the flow direction is negligible. α is the volume-averaged heat transfer coefficient for the structure.
  This assumption holds if the Biot number is much smaller than 1:

$$Bi = \frac{\alpha(t_{wall}/2)}{\lambda_s} \ll 1. \tag{4}$$

  The above criterion is met by all examined structures in this work, due to the small wall thickness of the metal foil and its relatively high thermal conductivity.
- Radiation effects within the channels are neglected.

These assumptions lead to the following energy balances, with α as the only unknown parameter, which describe the heat transfer between solid and fluid:

$$Fluid: \quad \frac{\partial T_f}{\partial t} = -v\frac{\partial T_f}{\partial x} + \alpha\frac{a}{\varepsilon\rho_f c_f}(T_s - T_f), \tag{5}$$

$$Solid: \quad \frac{\partial T_s}{\partial t} = -\alpha\frac{a}{(1-\varepsilon)\rho_s c_s}(T_s - T_f). \tag{6}$$

These two coupled, partial differential equations can be solved numerically by applying initial and boundary conditions.

If the packing is at steady state at $t = 0$, the initial condition is:

$$T_f = T_s = T_0 \quad \text{at } t = 0, \ 0 \leqslant x \leqslant L. \tag{7}$$

The *fluid equation* is of first-order and requires the specification of one boundary condition:

$$x = 0 : T_f = f(t), \tag{8}$$

where $f(t)$ is the function describing the step-like temperature change at the inlet of the packing with respect to time.

The heat transfer coefficient α is calculated with Eq. (9):

$$\alpha = \frac{Nu\,\lambda_f}{d_h} \ (\mathrm{W/m^2\ K}). \tag{9}$$

A commonly used correlation to describe the internal heat transfer in packed bed reactors is:

$$Nu = \not{c}\, Re^m Pr^n. \tag{10}$$

The values for ϕ and m depend on the type of flow and inner structure of the packing and must be determined individually for every type of packing. The value for the exponent n of the Pr number is set to $n = 1/3$ according to the literature [8]. This value has been used in all cases, as the Prandtl number for air does not change significantly over the range of test conditions.

2.3.1. Numerical procedure

Both parameters ϕ and m in Eq. (10) have to be determined such that calculated and measured temperature profiles (as a function of time) at the outlet of the packing agree over the entire range of Reynolds numbers. According to the iterative scheme shown in Table 3, both parameters are changed until the best matching set of ϕ and m for a particular packing is found.

An iterative process is necessary since a single experiment with constant air flow is not sufficient to determine ϕ and m simultaneously. With constant air flow during each particular experiment the Reynolds number and Re^m vary only weakly due to temperature changes.

The criterion used in judging the correctness of the calculations is the deviation of temperature gradient at the mean temperature of the experiment ($T_{\text{mean}} \cong$ 160–170 °C). Earlier studies have shown that this criterion is unambiguous and sufficient for this purpose [7]. Fig. 5 shows both calculated and measured outlet temperature profiles for a 150 cpsi Herringbone TI packing.

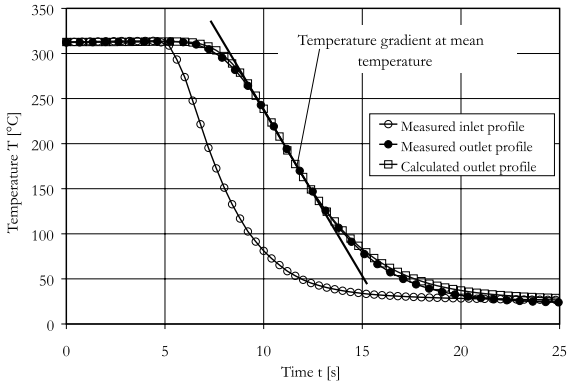

Fig. 5. Comparison of the measured and calculated outlet temperature profiles for a 150 cpsi Herringbone TI at a mass flow of 15 g/s ($\phi = 1.15$, $m = 0.27$). The agreement of the slope of the temperature curve at the mean temperature was used as the criterion for the curve fit.

Table 3
Iteration process for the derivation of a set of parameters ϕ and m

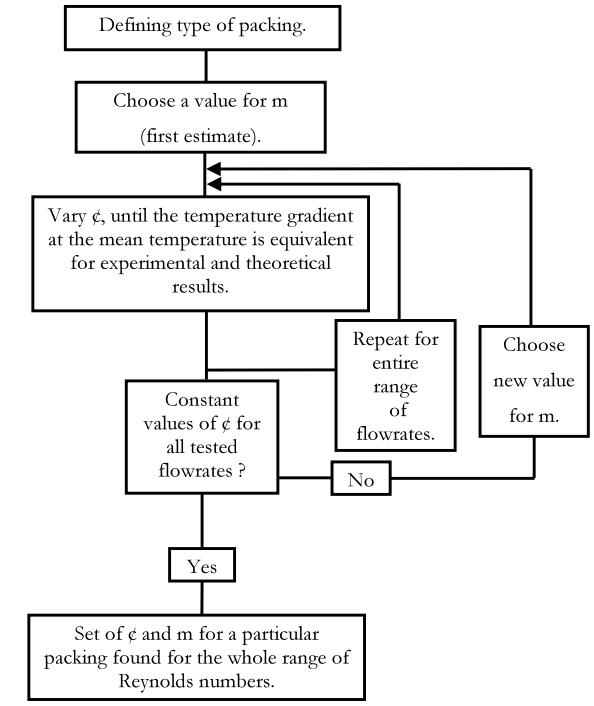

The above method for the measurement of heat transfer coefficients in packed beds is validated by applying it to measurements in a ceramic (Cordierite) honeycomb monolith. In these monoliths, the flow is laminar and heat transfer coefficients are well known from the literature [3,4]. The deviation between measured values and the literature data is less than 3%.

3. Results and discussion

3.1. Heat transfer

Table 4 shows the values for ϕ and m in Eq. (10) for the examined structures and the range of Reynolds numbers investigated. The geometrical data of each packing is summarized in Table 1.

A comparison of the above mentioned structures and the 400 cpsi monolith is shown in Fig. 6. Individually measured Nu values of the different tests are represented as separate points. The measurements are described accurately over the entire range of Re by the correlation given in Eq. (10). The maximum deviation is at most 5.7%, the mean deviation of all tests is 2.1%.

Fig. 6 shows that structures with higher cell densities yield smaller Nusselt numbers. Herringbone structures give higher Nusselt numbers for similar Reynolds numbers compared to the Skew pattern type. The novel Herringbone APT SK structure yields results comparable to the commercial Herringbone structures.

Table 4
Re number ranges and values ϕ and *m* for the examined packings

Structure type	*Re* (dimensionless)	ϕ (dimensionless)	*m* (dimensionless)
100 cpsi HB TI	380–1560	1.13	0.28
150 cpsi HB TI	290–950	1.15	0.27
200 cpsi HB TI	210–1130	1.19	0.21
100 cpsi SP TI	270–1250	1.08	0.25
160 cpsi HB APT SK	240–1130	1.21	0.23

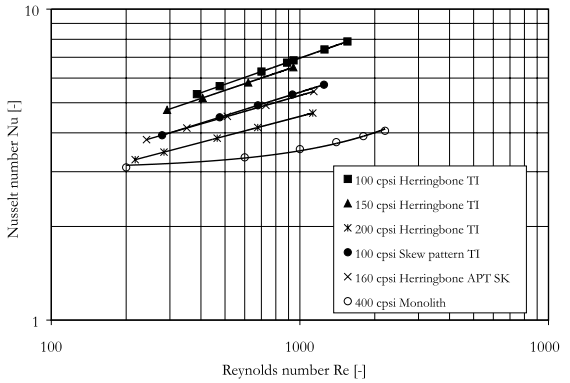

Fig. 6. *Nu* numbers as a function of *Re* numbers according to Eq. (10) for the examined packings. All fluid properties correspond to the mean temperature in the experiments of 160 °C.

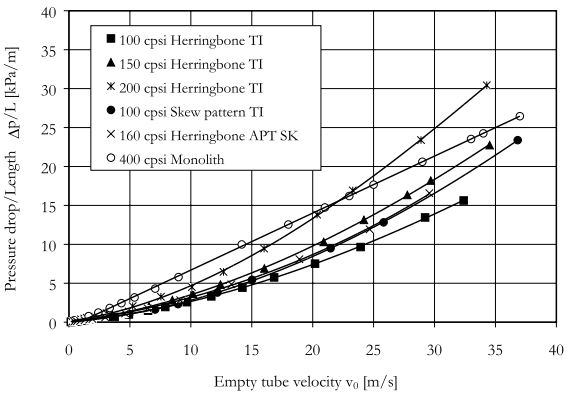

Fig. 7. Pressure drop Δp as a function of the empty tube velocity v_0 (related to a length of 1 m, a fluid temperature of 20 °C and D_{eff}).

The value of the exponent *m* in Eq. (10) is to some extent a measure of the level of turbulence in the support structure. An entirely turbulent flow pattern in tubes or packed beds has an *m* value of approximately 0.8, compared to a laminar flow with *m* values between 0 and 0.5 [4]. All tested packings have, according to the *m* value, a weakly turbulent flow pattern ($m = 0.21, \ldots,$ 0.28). As expected, finer structures (those with smaller channels) have an increased laminar flow character.

3.2. Pressure drop

Measured pressure drop per unit length is indicated in Fig. 7 for air at 20 °C and atmospheric pressure.

As expected, the dependency of the pressure drop per unit length for the monolith is linear, due to the laminar nature of the flow. In contrast for the Herringbone and Skew pattern structures, a slight departure from linearity is observed, an indication of turbulence in the flow. A comparison of different cell densities of the metal foil patterns shows an increase of pressure drop with cell density, with the 200 cpsi Herringbone having the highest values.

Skew pattern structures yield slightly higher pressure drops than Herringbone packings of similar cell densities. Because of the improved design (with less abrupt changes in corrugation angle) the self-made structure shows lower pressure drop than the equivalent packing made from commercial Herringbone foil.

3.3. Determination of structure transport "efficiency"

Knowledge of mass and heat transport characteristics of catalyst support structures is necessary for their optimal use in chemical processes such as catalytic combustion. In any heterogeneous catalytic process, reactants must be transported from the bulk to the catalyst surface where chemical reaction takes place. This means that the catalytic reaction cannot occur at a rate greater than that of either transport or the intrinsic surface reaction. The dependencies of both transport and catalytic reaction rate on temperature and reactant concentration lead to two simplified operating regimes in which either transport or chemical reaction is dominant [8].

3.3.1. Diffusion-controlled regime

In the diffusion controlled regime the reaction rate on the catalyst surface is much higher than the corresponding diffusive transport rate of reactants to the surface. This occurs in the case of high surface temperature where Arrhenius kinetics lead to extremely high surface reaction rates. Thus, the overall reaction rate is dependent on diffusion and thus only weakly dependent on the operating temperature.

3.3.2. Kinetically controlled regime

The kinetically controlled regime is found at lower surface temperatures, where the reaction rate is much lower. In this case the reaction rate is strongly dependent on the surface temperature (Arrhenius-type kinetics) and independent of diffusion.

According to these definitions, the reaction rate per unit volume in a catalytic reactor can be described as follows (via the analogy of heat and mass transfer, heat transfer coefficients can be used instead of mass transfer coefficients as the result is qualitatively the same):

"Reaction rate" per volume in the diffusion controlled regime:

$$q \sim \alpha a (\mathrm{W/m^3\ K}). \tag{11}$$

"Reaction rate" per volume in the kinetically controlled regime:

$$q \sim a (\mathrm{m^2/m^3}), \tag{12}$$

where a is the specific surface of the packing.

Fig. 8 shows the "reaction rate" in the diffusion controlled regime as a function of the empty tube velocity v_0 for the examined packings. For comparison, corresponding values for a 400 cpsi parallel-channel honeycomb are also shown.

Only packings with the highest cell densities (150 and 200 cpsi) allow for higher "reaction rates" than the 400 cpsi parallel-channel monolith. However, metal foil structures, if manufactured with similar cell densities as the 400 cpsi monolith, are expected to perform much better.

"Reaction rates" in the kinetically controlled regime depend on the specific surface area only (at a constant surface temperature) and are independent of the flow velocity. Therefore, none of the investigated structures could compete with a 400 cpsi honeycomb monolith (see Table 1). However, metal foil structures could be manufactured with higher cell densities and correspondingly higher surface areas.

The usefulness of a given catalyst support is not determined by its reaction rate alone, but also by its resistance to flow, expressed as a pressure drop. To rate the investigated structures in terms of an overall "efficiency", the reaction rate should be normalized with pressure losses.

In Figs. 9 and 10, normalized reaction rates for the diffusion and kinetically limited regimes are compared with results for a 400 cpsi parallel-channel honeycomb. In all cases the pressure drops have been referenced to $L = 0.1$ m and air properties at 20 °C.

All of the examined packings yield similar curves of the reaction rates per pressure drop vs. the empty tube velocity (in the diffusion controlled as well as in the kinetically controlled regime). This means that for all

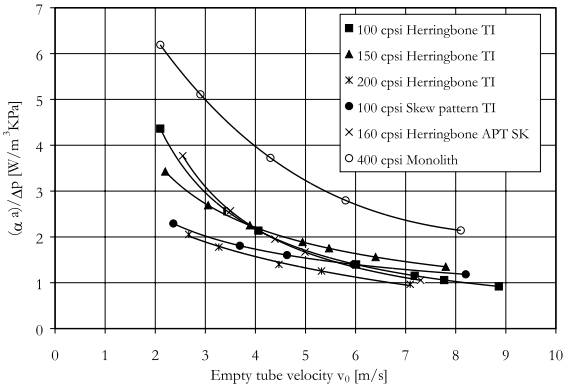

Fig. 9. "Reaction rate" in the diffusion limited regime per pressure drop ($\alpha a/\Delta p$) as a function of the empty tube velocity (related to a fluid temperature of 20 °C, D_{eff} and $L = 0.1$ m).

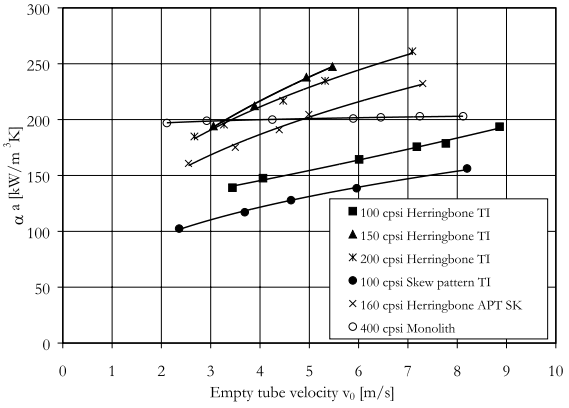

Fig. 8. "Reaction rate" in the diffusion controlled regime (αa) as a function of the empty tube velocity v_0 (related to a fluid temperature of 20 °C and D_{eff}; $L = 0.1$ m).

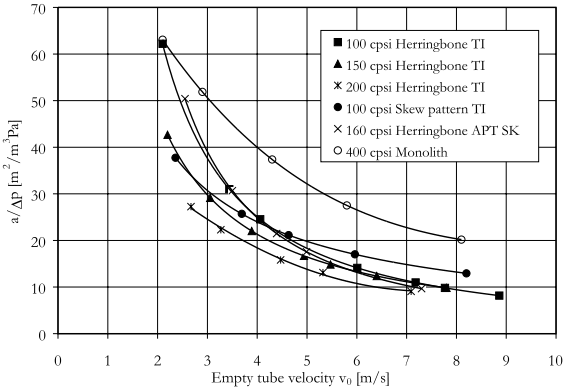

Fig. 10. "Reaction rate" in the kinetically limited regime per pressure drop ($a/\Delta p$) as a function of the empty tube velocity (related to a fluid temperature of 20 °C, D_{eff} and $L = 0.1$ m).

packings higher reaction rates are penalized with increased pressure drop. The most "efficient" performance is seen at low air velocities where the flow is less turbulent. At high velocities (>6 m/s) all packings are roughly equivalent in their efficiency and the choice of cell density leads simply to a variation in the overall catalyst reactor volume. In both reaction regimes the investigated metal foil packings are significantly less efficient than a 400 cpsi Cordierite honeycomb. This means that the advantages of higher heat transfer rates in these structures are significantly outweighed by the correspondingly higher pressure drop per unit length.

4. Conclusion

Despite its simplicity, the measurement method described in this paper delivers reliable values for convective heat transfer coefficients in novel metal foil catalyst supports. The expression $Nu = \phi Re^m Pr^{1/3}$ is suitable for describing heat transfer between the solid surfaces and the heat transfer medium (in this case air). The measured Nusselt numbers and associated heat transfer coefficients (α (W/m^2)) for the investigated support structures vary over a wide range, depending on the cell density and channel shape, and are greater than those for a 400 cpsi parallel-channel, Cordierite honeycomb. However, the efficiency of heat transfer (quantified by the normalization of the heat transfer coefficients to pressure drop) of the investigated metal foil structures are similar to each other and are significantly worse than that of the 400 cpsi honeycomb. Thus, while corrugated metal foil structures offer increased heat and mass transfer per unit volume, this advantage must be "paid for" by the greater increase in pressure drop.

Despite these shortcomings, the investigated packings offer performance advantages for particular applications due to:

- Possibility of radial mixing between channels of a particular layer in the structure to even out incoming concentration and temperature profiles to avoid/reduce the intensity of hot spots.
- Reduction of overall reactor volume due to greater transport rates per unit volume.

Ongoing work is being performed to take advantage of these features in new structural designs, with higher cell density, smaller departure of the corrugation angle from the flow direction, and the use of holes in the foil to enhance channel-to-channel mixing. The method described in this paper for rapid and simple measurements of heat transfer coefficients will be employed to aid the authors in this optimization process.

References

[1] R. Hayes, S. Kolaczkowski, Introduction to Catalytic Combustion, Gordon and Breach, London, 1997.
[2] A. Schlegel, P. Benz, T. Griffin, W. Weisenstein, H. Bockhorn, Catalytic stabilization of lean premixed combustion: method for improving NO_x-emissions, Combust. Flame 105 (1996) 332–340.
[3] W.M. Rohsenow, J.P. Hartnett, Handbook of Heat Transfer, McGraw-Hill, New York, 1973.
[4] VDI-Wärmeatlas, 4. Auflage, VDI Verlag, Düsseldorf, 1984.
[5] E.U. Schlünder, Wärmeübertragung in Festbetten, durchmischten Schüttgütern and Wirbelschichten, Georg Thieme Verlag, Stuttgart, 1988.
[6] A. Schlegel, P. Benz, S. Buser, Wärmeübertragung und Druckabfall in keramischen Schaumstrukturen bei erzwungener Strömung, Wärme- Stoffübertrag. 28 (1993) 259–266.
[7] A. Schlegel, P. Benz, S. Buser, Bestimmung der Wärmeübergangskoeffizienten in keramischen Schaumstrukturen, Technische Mitteilung (TM-51-91-05), Paul Scherrer Institut, CH-5232 Villigen PSI, Switzerland, 1991.
[8] D.E. Rosner, Transport Processes in Chemically Reacting Flow Systems, Butterworth, Stoneham, USA, 1986.